Determination of the Transbilayer Distribution of Fluorescent Lipid Analogues by Nonradiative Fluorescence Resonance Energy Transfer†

David E. Wolf,*,‡ Anthony P. Winiski,§ Anthony E. Ting,§ Kristine M. Bocian,‡ and Richard E. Pagano§

Worcester Foundation for Experimental Biology, 222 Maple Avenue, Shrewsbury, Massachusetts 01545, and Carnegie Institution of Washington, Department of Embryology, 115 University Parkway, Baltimore, Maryland 21210

Received September 11, 1991; Revised Manuscript Received December 17, 1991

ABSTRACT: We measured the nonradiative fluorescence resonance energy transfer between 7-nitro-2,1,3-benzoxadiazol-4-yl (NBD) labeled lipids (amine labeled phosphatidylethanolamine or acyl chain labeled phosphatidylcholine) and rhodamine labeled lipids in large unilamellar dioleoylphosphatidylcholine vesicles. Two new rhodamine labeled lipid analogues, one a derivative of monolauroylphosphatidylethanolamine and the other of sphingosylphosphorylcholine, were found to exchange through the aqueous phase between vesicle populations but not to be capable of rapid transbilayer movement between leaflets. Energy transfer from NBD to rhodamine was measured using liposomes with symmetric or asymmetric distributions of these new rhodamine labeled lipid analogues to determine the relative contributions of energy transfer between donor and acceptor fluorophores in the same (cis) and opposite (trans) leaflets. Since the characteristic R_0 values for energy transfer ranged from 47 to 73 Å in all cases, significant contributions from both cis and trans energy transfer were observed. Therefore, neither of these probes acts strictly as a half-bilayer quencher of NBD lipid fluorescence. The dependence of transfer efficiency on acceptor density was fitted to a theoretical treatment of energy transfer to determine the distances of closest approach for cis and trans transfer. These parameters set limits on the positions of the fluorescent groups relative to the bilayer center, 20–31 Å for NBD and 31–55 Å for rhodamine, and provide a basis for future use of these analogues in measurements of transbilayer distribution and transport.

Fluorescent lipids have been used to study both biological and model membrane systems (Loew, 1988). One widely used class of fluorescent lipid analogues are the 7-nitro-2,1,3-benzoxadiazol-4-yl (NBD)[1] labeled lipids (Pagano & Sleight, 1985; Chattopadhyay, 1990). A useful property of NBD is that it can transfer excited state energy by nonradiative fluorescence resonance energy transfer (FRET) with lissamine rhodamine (LRH) and sulforhodamine (SRH) lipid analogues (Struck et al., 1981; Nichols & Pagano, 1982, 1983; Uster & Pagano, 1986; Connor & Schroit, 1987). FRET involves the transfer of energy from one fluorophore (the donor) to another (the acceptor) by a dipole-induced dipole interaction (Förster, 1948). FRET manifests itself in several phenomena: quenching and depolarization of donor steady-state fluorescence, sensitized emission of acceptor fluorescence, and shortening of donor excited state lifetime. Transfer efficiency (E_T) decreases as the sixth power of the reciprocal of the interfluorophore distance. Thus, FRET is exquisitely sensitive to distance and has been called "the spectroscopic ruler" (Stryer, 1974).

This spatial sensitivity has been exploited to obtain three-dimensional structural information about biomolecules. For example, it has been used to study the structure of polynucleotide hybridization (Cardullo et al., 1988), to measure receptor aggregation and the structure of ligand–receptor complexes in membranes (Dale et al., 1980; Baird & Holowka, 1988), to determine the structure of proteins in membranes (Kleinfeld, 1985), and to study the polymerization and structure of biopolymers such as actin (Taylor et al., 1981; Tao et al., 1983).

Beyond applications of FRET in spectrofluorimetric studies, it can be employed at the single-cell level in cell sorting experiments and in fluorescence microscopy (Uster & Pagano, 1986). FRET has been used to measure the transport of NBD lipids between lipid vesicles (Nichols & Pagano, 1982, 1983) and to test the ability of NBD lipids to undergo transbilayer movement ("flip-flop") (Pagano & Longmuir, 1985; Pagano, 1989; Conner & Schroit, 1987). However, the use of FRET to determine transbilayer distribution and measure the transport within cells has been hampered by the lack of exchangeable acceptor lipid analogues which do not themselves flip across membranes. In this paper, we introduce LRH and SRH lipid analogues that exchange between membranes but do not flip-flop across lipid bilayers. These properties allowed us to selectively place the exchangeable LRH and SRH lipid analogues in either the inner and/or outer leaflet of lipid

† This work was supported in part by Research Grants HD23294 (D.E.W.) and R37-GM22942 (R.E.P.) from the U.S. Public Health Service. Additional support was provided by the Whitaker Foundation (D.E.W.) and by a grant from the A. W. Mellon Foundation to the Worcester Foundation. A.P.W. was supported by a National Institutes of Health postdoctoral fellowship.

* To whom correspondence should be addressed.
‡ Worcester Foundation for Experimental Biology.
§ Carnegie Institution of Washington.

[1] Abbreviations: C_6-NBD-PC, 1-palmitoyl-2-(NBD-aminocaproyl)-phosphatidylcholine; D, doublet, S, single band; DOPC, dioleoylphosphatidylcholine; FRET, nonradiative fluorescence resonance energy transfer; LRH, lissamine rhodamine; MLPE, monolauroylphosphatidylethanolamine; NaCl-HEPES, 0.9% NaCl in 10 mM 4-(2-hydroxyethyl)-1-piperazineethanesulfonic acid, pH 7.4; NBD, 7-nitro-2,1,3-benzoxadiazol-4-yl; *N*-NBD-PE, egg *N*-NBD-phosphatidylethanolamine; *N*-LRH-MLPE, *N*-LRH-monolauroylphosphatidylethanolamine; *N*-LRH-PE, egg *N*-LRH-phosphatidylethanolamine; *N*-SRH-PE, *N*-SRH-dioleoylphosphatidylethanolamine; *N*-SRH-SPC, *N*-SRH-sphingosylphosphorylcholine; SPC, sphingosylphosphorylcholine; SRH; sulforhodamine.

0006-2960/92/0431-2865$03.00/0

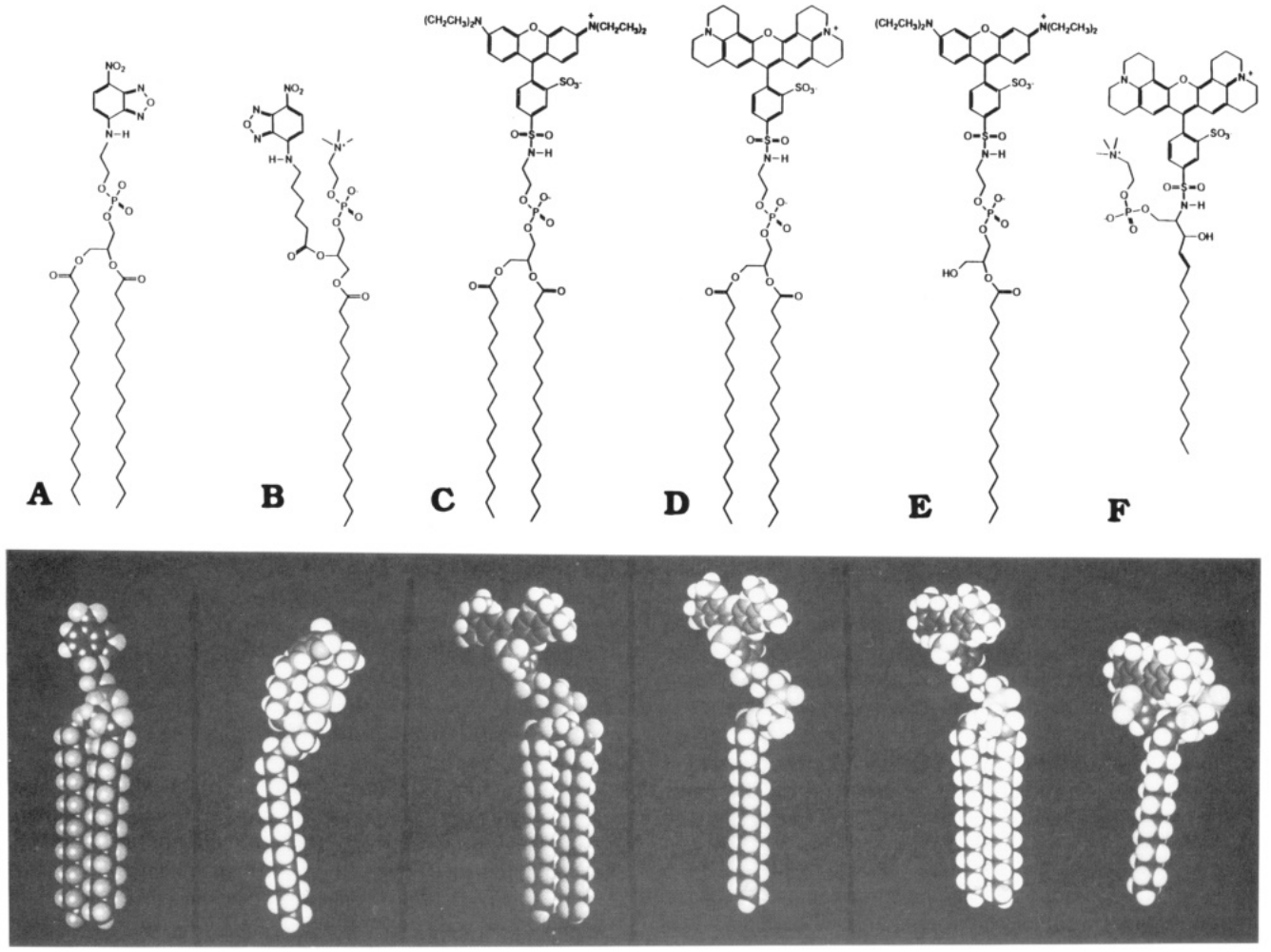

FIGURE 1: (Top) Structures of fluorescent lipid analogues used in this study. (A) *N*-NBD-PE. (B) C_6-NBD-PC. (C) *N*-LRH-PE. (D) *N*-SRH-PE. (E) *N*-LRH-MLPE. (F) *N*-SRH-SPC. (Bottom) Corresponding 3D structures generated using the DISCOVER energy minimization program (see Materials and Methods). Structures are arranged by aligning the phosphates and indicate positions in the bilayer which are consistent with Table II model were $a = d_{cis}$.

vesicles, which also contained nonexchangeable NBD lipid. We were thus able to determine the relative contributions of energy transfer between NBD and rhodamine acceptor fluorophores in the same (cis) and opposite (trans) leaflets. These measurements provide a basis for future applications, including measurement of lipid flip-flop at the plasma membrane of living cells and subsequent transport of NBD lipids to intracellular membranes.

Materials and Methods

Lipids. The structures of the fluorescent lipid analogues used in this study are shown in Figure 1. Dioleoylphosphatidylcholine (DOPC), L-α-monolauroylphosphatidylethanolamine (MLPE), egg *N*-(7-nitro-2,1,3-benzoxadiazol-4-yl)phosphatidylethanolamine (*N*-NBD-PE), *N*-LRH-PE, *N*-SRH-PE, and 1-palmitoyl-2-(C_6-NBD)PC (C_6-NBD-PC) were obtained from Avanti Biochemicals (Pelham, AL). All lipids were analyzed on silica gel TLC, purified as required, and stored in organic solvent at −20 °C. Lipid phosphorus concentrations were determined according to Rouser et al. (1970). 4-(2-hydroxyethyl)-1-piperazineethanesulfonic acid (HEPES) was obtained from Research Organics, Inc. (Cleveland, OH). Sphingosylphosphorylcholine (SPC) was obtained from Sigma (St. Louis, MO). Lissamine rhodamine sulfonyl chloride and sulforhodamine sulfonyl chloride (Texas Red) were obtained from Molecular Probes (Eugene, OR).

Preparation of Exchangeable Rhodamine Labeled Lipids. A lissamine rhodamine derivative of MLPE (*N*-LRH-MLPE) was synthesized as follows. Triethylamine (30 μL) (Aldrich, Milwaukee, WI) was added to 5 mg of MLPE dissolved in 0.5 mL of CH_3OH. Lissamine rhodamine sulfonyl chloride (36 mg) in 0.45 mL of CH_3OH was added, and the reaction mixture was stirred for 3 h at room temperature in the dark. The reaction mixture was dried under N_2, dissolved in $CHCl_3/CH_3OH$ (1:1), and separated by silica gel 60 (EM Science, Cherry Hill, NJ) TLC using $CHCl_3/CH_3OH$/28% aqueous NH_4OH (65:35:5) as the developing solvent. One unique fluorescent product (R_f = 0.49) was identified compared to a mock reaction mixture lacking MLPE. The *N*-LRH-MLPE was scraped, extracted, dried under N_2, and twice purified by consecutive preparative TLC using $CHCl_3/CH_3OH/H_2O$/acetone/acetic acid (50:10:5:20:10) as the developing solvent (R_f = 0.2). The final yield of *N*-LRH-MLPE as determined by fluorescence measurements was ~20%.

N-SRH-SPC, a sulforhodamine derivative of SPC, was prepared by first adding 300 μL of triethylamine to 50 mg of SPC in 3 mL of $CHCl_3$. Sulforhodamine sulfonyl chloride (80 mg) in 5 mL of CH_3OH was then added. After the reaction mixture was stirred for 3 h at room temperature in

the dark, 8 mL of $CHCl_3$ and 7.2 mL of acidic saline (0.9% NaCl, 15 mM HCl) were added. The reaction mixture was vortex mixed, centrifuged, and the upper aqueous phase discarded. The lower organic phase was washed three times with an equal volume of CH_3OH/acidic saline (1:1), dried under N_2, dissolved in $CHCl_3/CH_3OH$ (10:1), and separated by TLC using $CHCl_3/CH_3OH$/28% aqueous NH_4OH/H_2O (72:48:2:9) as the developing solvent. When compared to a mock reaction mixture lacking SPC, two unique fluorescent products were identified, a single band (R_f = 0.36) referred to as *N*-SRH-SPC(S) and a doublet ($R_f \sim 0.3$) termed *N*-SRH-SPC(D). The *N*-SRH-SPC isomers were scraped, extracted, and further purified using C18 reverse-phase TLC plates (Whatman, Clifton, NJ) using $CHCl_3/CH_3OH/H_2O$ (1:3:1) as the mobile phase [R_f = 0.16 and 0.13 for *N*-SRH-SPC(S) and (D), respectively]. This was followed by an additional separation by TLC with $CHCl_3/CH_3OH$/28% aqueous NH_4OH/H_2O (72:48:2:9) (R_f values, see above). The yields of *N*-SRH-SPC(S) and *N*-SRH-SPC(D) were determined by fluorescent measurements and were ~2% and ~1%, respectively. The presence of *N*-SRH-SPC isomers probably resulted from both the starting SPC and sulforhodamine sulfonyl chloride having at least two different isomers each.

The structures of all the rhodamine lipid products were confirmed by mass spectrometry, which was carried out at the Middle Atlantic Mass Spectrometry Laboratory, a National Science Foundation Shared Instrumentation Facility. *N*-LRH-MLPE in methanol had a molar extinction coefficient of 137 000 M^{-1} cm^{-1} at 560 nm and exhibited fluorescence excitation and emission peaks at 572 and 590 nm, respectively, in DOPC liposomes at 0.5 mol %. *N*-SRH-SPC(S) in methanol had a molar extinction coefficient of 118 000 M^{-1} cm^{-1} at 584 nm and exhibited fluorescence excitation and emission peaks at 593 and 608 nm, respectively, in DOPC liposomes at 0.5 mol %.

Fluorescence Measurements. Steady-state fluorescence was measured at magic angle orientation (54.7°) at 530 nm (λ_{ex} = 470 nm) for NBD-lipids, at 590 nm (λ_{ex} = 535 nm) for lissamine rhodamine-lipids, and at 605 nm (λ_{ex} = 550 nm) for sulforhodamine lipids with an SLM-8000C fluorimeter (Urbana, IL) in the photon-counting mode. All measurements were made at 25 °C using polystyrene cuvettes (10 × 10 × 48 mm) from Sarstedt (Princeton, NJ).

Preparation of Lipid Vesicles. The following two methods were employed to prepare unilamellar vesicles. (i) Large unilamellar vesicles (LUVs) ~1000 Å in diameter were prepared by ethanol injection (Kremer et al., 1977). A lipid mixture in ethanol (32 mM) was injected into a solution of 10 mM HEPES, pH 7.4, and 0.9% NaCl (NaCl-HEPES). The resulting LUVs were then diluted with NaCl-HEPES to a final concentration of 16 μM lipid. (ii) Large unilamellar vesicles were also prepared by the extrusion technique (LUVETS) (Hope et al., 1985; Mayer et al., 1985). Briefly, DOPC was dried under nitrogen, desiccated in vacuo, and redispersed using a vortex mixer into NaCl-HEPES to produce multilamellar vesicles. These vesicles were then exposed to five cycles of freezing in liquid N_2 and thawing at 40 °C. The vesicles were then extruded 10 times through two stacked 0.1-μm polycarbonate filters to produce LUVETS of ~1000 Å in diameter at concentrations of 10–50 mM.

To prepare vesicles with a symmetric distribution of a given probe, the probe was added to the lipid mixture prior to formation of membranes. To prepare vesicles with an asymmetric distribution of an exchangeable probe, two methods where used: (1) the outer leaflet of initially symmetric vesicles was diluted by incubation with unlabeled vesicles or (2) probe was added from the aqueous phase to the outer leaflet of preformed membranes.

Three types of vesicles were used in these experiments:

Vesicles Containing N-NBD-PE or C_6-NBD-PC in Both Leaflets and Rhodamine Lipid in either Both Leaflets (Type I) or Only in the Inner Leaflet (Type II). We prepared DOPC LUVs (16 μM) containing 1 mol % *N*-NBD-PE or C_6-NBD-PC and 0–5 mol % rhodamine lipid in both leaflets by the ethanol injection method. The relative NBD fluorescence was first measured for the sample, DOPC LUVETS were added to a 70-fold molar excess from a concentrated stock solution, and NBD fluorescence was again measured. The small contribution of light scattering due to the added LUVETS was subtracted from each measurement. Finally, Triton X-100 was added to 1% (v/v), and both NBD and rhodamine fluorescence were measured. Triton disrupts the vesicles, thus separating the NBD and rhodamine labeled lipids, eliminating energy transfer. These measurements with Triton provided a calibration for the concentration determination of both NBD and rhodamine labeled lipids with the asymmetric vesicles described below.

Vesicles Containing N-NBD-PE in Both Leaflets and Rhodamine Lipid in Only the Outer Leaflet (Type III). We parpared DOPC LUVs (16 μM) containing 1 mol % *N*-NBD-PE in both leaflets. The NBD fluorescence was measured and aliquots of exchangeable rhodamine lipid were added from a concentrated solution in NaCl-HEPES to individual LUV samples to produce vesicles containing rhodamine lipid in the outer leaflet at ~0–4 mol %, and NBD fluorescence was measured. Finally, Triton X-100 was added to 1% (v/v), and both NBD and rhodamine fluorescence were measured. The mole percents of rhodamine lipid in the outer leaflet were determined from the rhodamine fluorescence in the presence of Triton X-100. These were compared to a calibration curve of rhodamine fluorescence (+ Triton X-100) vs mole percent rhodamine lipid generated from the symmetric vesicle experiment described above and multiplied by two to account for outer leaflet-only labeling. All fluorescence measurements described above were performed on the same day. The experiments were done at sufficiently low optical densities to avoid inner filter effects. All changes in fluorescence intensity which resulted from addition of exchangeable rhodamine lipids, DOPC LUVETS, or Triton X-100 were found to be complete by the end of the mixing procedure (~30 s).

Resonance Energy Transfer Calculations. Resonance energy transfer efficiency (E_T) of the various vesicle populations was determined by assessing the degree of NBD fluorescence quenching. Briefly, vesicles (16 μM DOPC LUVs) containing constant concentrations of *N*-NBD-PE (1 mol %) and increasing concentrations of rhodamine lipid (0–5 mol %) in either both leaflets or only in one leaflet were prepared as described above, and the relative NBD fluorescence was determined in the absence and presence of 1% Triton X-100.

E_T was calculated as

$$1 - (F/F_0)(F_0^{+TX}/F^{+TX}) \quad (1)$$

where F and F_0 were the relative NBD fluorescences in LUVS with or without the rhodamine lipid, respectively. The +TX superscripts designate the presence of Triton X-100. Thus, (F_0^{+TX}/F^{+TX}) is a correction factor for variations in the amount of NBD lipid. In a typical experiment, this correction factor varies by about 12% (SD) from 1.0.

Analysis of FRET Data. FRET data were analyzed by a modification of the theory of Fung and Stryer (1978). For an isolated donor–acceptor pair separated by a distance r, the rate of energy transfer k_T is given by

$$k_T = \left(\frac{1}{\tau_0}\right)\left(\frac{R_0}{r}\right)^6 \quad (2)$$

where τ_0 is the donor's excited state lifetime in the absence of acceptor and R_0 is the distance where the transfer efficiency is 0.50.

R_0 in angstroms can be calculated from first principles

$$R_0 = (J\kappa^2 Q_0 n^{-4})^{1/6} \times 9.786 \times 10^3 \quad (3)$$

where Q_0 is the quantum yield of donor in the absence of acceptor, n is the index of refraction, κ^2 is the dipole–dipole orientation factor, and J is the overlap integral given by

$$J = \int_0^\infty A(\lambda)E(\lambda)\lambda^4\, d\lambda / \int_0^\infty E(\lambda)\, d\lambda \quad (4)$$

where $A(\lambda)$ is the absorbance spectrum of acceptor (M^{-1} cm^{-1}) as a function of wavelength, λ, and $E(\lambda)$ is the corrected fluorescence emission spectrum of donor.

In the presence of energy transfer, the probability $p(t)$ that a donor molecule in the excited state at time 0 is still in the excited state at time t is given by

$$p(t) = \exp(-t/\tau_0)\exp(-k_T t) \quad (5)$$

The transfer efficiency is then defined as

$$E_t = 1 - \int_0^\infty p(t)\, dt / \int_0^\infty p_0(t)\, dt \quad (6)$$

where $p_0(t)$ is $p(t)$ in the absence of acceptor (i.e., $k_T = 0$). Equation 6 thus reduces to eq 1 without the correction factor.

Transfer among fluorescent lipid probes in a bilayer is not between an isolated donor–acceptor pair but between a donor and a distribution of acceptors. Figure 2 shows the essential elements of this process. If the donor fluorophore is at distance x from the bilayer center, the fluorophore can transfer energy in the plane of the bilayer (cis transfer) to an acceptor group at a distance y above the bilayer center, or it can transfer energy to an acceptor in the opposite leaflet transfer which is also a distance y from the center. Equation 5 then becomes

$$p(t) = \exp(-t/t_0)\exp[-\sigma(S_{cis} + S_{trans})] \quad (7)$$

where

$$S_{cis} \equiv \int_a^\infty [1 - \exp(-t/\tau_0)(R_0/r)^6]2\pi z\, dz \quad (8a)$$

$$S_{trans} \equiv \int_b^\infty [1 - \exp(-t/\tau_0)(R_0/r)^6]2\pi z\, dz \quad (8b)$$

and where σ is the density of acceptors in each leaflet. z is a variable of integration in the plane of the bilayer. For cis transfer

$$z^2 = r^2 - (y - x)^2 \quad (9a)$$

and for trans transfer

$$z^2 = r^2 - (y + x)^2 \quad (9b)$$

a and b are the distances of closest approach for cis and trans transfer respectively. Steric hindrance would be expected to prevent the fluorophores from coming any closer than a distance a in the plane. However, steric effects should not be an issue in the case of trans transfer, and the acceptor could be immediately below the donor. Thus $b = 0$. It is convenient, as pointed out by Fung and Styer (1978), to make a change of variables so as to be able to integrate over r. We note for both eqs 9a and 9b that

$$2\pi z\, dz = 2\pi r\, dr \quad (10)$$

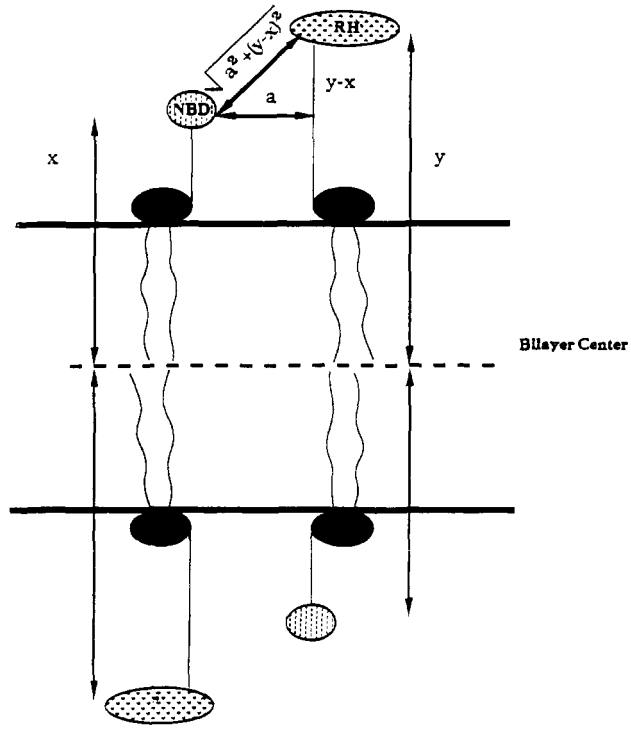

FIGURE 2: Schematic diagram of model used to fit the FRET data. Donor NBD groups are assumed to be equally distributed between the two leaflets at a distance x from the bilayer center. Acceptor (RH) groups are a distance y from the bilayer center. Their distribution between leaflets depends upon the experiment. It is assumed that within the plane of the membrane there is a distance (a) of closest approach and that across the bilayer an RH group in one leaflet can get directly below an NBD group in the opposite leaflet. Thus, the distance of closest approach for cis transfer is $[a^2 + (y - x)^2]^{1/2}$ and for trans transfer is $(x + y)$.

Thus eqs 8a and 8b become

$$S_{cis} = \int_{\sqrt{a^2 + (y-x)^2}}^\infty [1 - \exp(-t/\tau_0)(R_0/r)^6]2\pi r\, dr \quad (11a)$$

$$S_{trans} = \int_{y+x}^\infty [1 - \exp(-t/\tau_0)(R_0/r)^6]2\pi r\, dr \quad (11b)$$

It should be noted that the above derivation does not assume that $y > x$ or that x and y are less than the bilayer half-thickness. Equation 7 describes the case in our experiments where donor and acceptor were equally distributed between the bilayer leaflets (case I: symmetric vesicles). In all cases considered, donor distribution remained equal while that of acceptor varied. The following cases were also considered.

Case II: *Symmetric Vesicles + DOPC*. Here the DOPC vesicles were added as a sink to dilute the distribution of acceptor in the outer leaflet 70-fold.

$$p(t) = 0.5\exp(-t/\tau_0) \times [\exp[-\sigma(S_{cis} + S_{trans}/70)] + \exp[-\sigma(S_{cis}/70 + S_{trans})]] \quad (12)$$

Case III: *Asymmetric Vesicles*. Here, acceptor was present only in the outer leaflet.

$$p(t) = 0.5\exp(-t/\tau_0)[\exp(-\sigma S_{cis}) + \exp(-\sigma S_{trans})] \quad (13)$$

Case IV: *Asymmetric Vesicles + DOPC*. Here as in case II the outer leaflet acceptor concentration was diluted 70-fold.

$$p(t) = 0.5\exp(t/\tau_0)[\exp(-\sigma S_{cis}/70) + \exp(-\sigma S_{trans}/70)] \quad (14)$$

Data from energy transfer experiments was reduced to transfer efficiency E_T vs mole fraction acceptor. These data were then fitted by minimization of χ^2 to eq 6 with the appropriate expression for $p(t)$ (eqs 7–14) using a grid search procedure (Bevington, 1969) and varying the two distances of closest approach and R_0. The integrations over space in the S terms and over time in eq 6 were performed using Gauss' approximation (Abramowitz & Stegun, 1965). Data were analyzed on a Compaq 386/20 with math coprocessor. Programs were written in MS Pascal. Alternatively, R_0 can be determined from first principles as described above and the data then fit to determine the two distances of closest approach only. This gave similar results. However, as we shall show there is considerable uncertainty in R_0 determinations from spectral data. Thus, parametric variations of R_0 were found to be preferable. Once a χ^2 minimum was obtained by grid search, a three-point parabolic fit of χ^2 around the best grid is made to obtain the minimum. Uncertainty in the parameters obtained was estimated from the second derivatives of χ^2 with respect to the parameters as described by Bevington (1969). Where more than one determination was made, the uncertainty reported was determined by error propagation of the individual uncertainties.

Generation of Three-Dimensional Molecular Structures. Three-dimensional molecular structures were generated on a Silicon Graphics IRIS 4D/340 VGXB Unix workstation with four 33-MHz IP 7 processors operating under IRIX 4D 1–3.3. Software used for this purpose was from Biosym Technologies (San Diego, CA): INSIGHT II version 2.0.0 comprehensive graphic molecular modeling program in conjunction with the DISCOVERY program for energy minimization.

RESULTS

Calculation of R_0 from First Principles. As shown in eq 3, R_0 may be calculated from the fundamental spectral properties of the donor and acceptor fluorophores. The following must be known: the corrected emission spectrum of the donor, the quantum efficiency of donor fluorescence, the absorbance spectrum of the acceptor, the orientation factor between the donor emission and acceptor absorbance dipoles, and the refractive index of the medium.

Donor Emission Spectrum and Quantum Efficiency. Figure 3 (top, dashed line) shows the corrected emission spectrum of *N*-NBD-PE in ethanol, when exciting at 366 nm. The spectrum is qualitatively the same in DOPC membranes but with a reduced quantum efficiency (see below).

To determine the quantum efficiencies of *N*-NBD-PE in ethanol and membranes, the area contained by the emission spectrum of the ethanol sample was compared to that of a standard solution of quinine bisulfate (2.55×10^{-6} M in 0.1 M H_2SO_4). Assuming the literature value of 0.55 for the quantum efficiency of quinine bisulphate under these conditions (Parker, 1968), we obtain a quantum efficiency of 0.39 for *N*-NBD-PE in ethanol. This value compares favorably with a value of 0.37 previously reported for NBD-benzylamine in ethanol (Kenner et al., 1971). Since the relative quantum efficiencies of *N*-NBD-PE in a membrane to that in ethanol was found to be 0.81, the quantum efficiency of *N*-NBD-PE in DOPC was 0.32.

Absorbance Spectra. Figure 3(bottom) shows the absorbance spectra for *N*-LRH-PE (solid line) and *N*-SRH-PE (dashed) in DOPC membranes at 1.0 mol %. For completeness, we also show the absorbance spectrum for *N*-NBD-PE in ethanol (Figure 3, top, solid line).

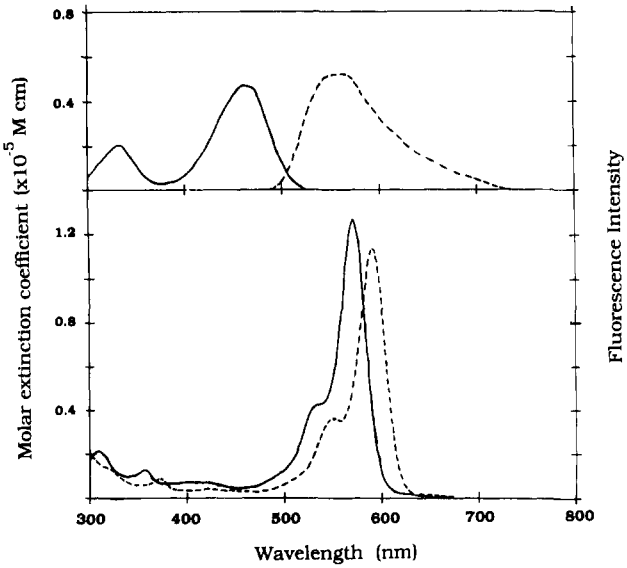

FIGURE 3: Spectra of the fluorophores used in these studies. (Top) (—) Absorbance spectrum of *N*-NBD-PE in ethanol; (---) corrected fluorescence emission spectrum of *N*-NBD-PE in ethanol with excitation at 366 nm. (Bottom) (—) Absorbance spectrum of *N*-LRH-PE (1 mol %) in DOPC membranes; (---) absorbance spectrum of *N*-SRH-PE (1 mol %) in DOPC membranes.

Calculation of R_0. Using the data of Figure 3 and eq 3, the overlap integrals for FRET between *N*-NBD-PE and *N*-LRH-PE and *N*-SRH-PE can be calculated. One can then calculate the predicted R_0 values for transfer between these two pairs if one uses the quantum efficiency from above and assumes that κ^2 is $^2/_3$ (Koppel, et al., 1978) and that the index of refraction for the medium is 1.33 (Weast et al., 1987). By this method, we calculate R_0 to be 56 and 55 Å for transfer from *N*-NBD-PE to *N*-LRH-PE and *N*-SRH-PE, respectively.

Acquisition of corrected spectra and quantum efficiencies is difficult, and there is not even total agreement on standards and standardized procedures (Mavrodineau et al., 1973). In addition, assuming κ^2 to be $^2/_3$ is an approximation. As a result, R_0 values so obtained must be considered as estimates. In the following experiments, we have therefore allowed R_0 to be a parameter in our fits of the data. This approach recognizes the fact that a FRET experiment represents a direct measurement of R_0. As we show below, this approach leads to a very self-consistent set of R_0's which can differ by as much as 30% from the predicted value at ~55 Å.

Energy Transfer Measurements. Results of energy transfer measurements are summarized in Table I with specific examples shown in Figure 4. In all cases, donor analogues, either *N*-NBD-PE or C_6-NBD-PC, were added to the lipid mixture before forming bilayers. We make two a priori assumptions: (1) that analogues added to the membrane-forming solutions equally distribute between the leaflets and (2) that these analogues do not flip between the leaflets. These assumptions have been shown to hold for C_6-NBD-PC (Pagano et al., 1981b), and their validity for the other NBD and rhodamine analogues used here is demonstrated by the experiments described below. Figure 4A shows energy transfer between *N*-NBD-PE and *N*-LRH-PE in symmetric vesicles as a function of acceptor concentration. Data were fit as described under Materials and Methods to determine R_0 and the distances of closest approach for cis and trans transfer (Table I, experiments 1 and 2). Both *N*-NBD-PE and *N*-LRH-PE do not exchange across the aqueous phase between lipid vesicles (Pagano et al., 1981b; Struck & Pagano, 1980). Thus, the addition of a 70-fold excess of DOPC vesicles did not alter

Table I: Depth of Probe Determined by Energy Transfer[a]

exp no.	donor	acceptor	±DOPC[b]	R_0 (Å)	distance of closest approach (Å) cis	distance of closest approach (Å) trans	eq
	Symmetric Vesicles: Nonexchangeable Acceptor						
1	*N*-NBD-PE	*N*-LRH-PE	−	69 ± 1	22 ± 5	62 ± 3	7
2	*N*-NBD-PE	*N*-LRH-PE	−	64 ± 1	22 ± 3	62 ± 3	7
3	*N*-NBD-PE	*N*-LRH-PE	+	64 ± 1	20 ± 4	62 ± 3	7
4	*N*-NBD-PE	*N*-SRH-PE	−	74 ± 4	42 ± 10	72 ± 14	7
5	*N*-NBD-PE	*N*-SRH-PE	−	71 ± 1	32 ± 2	73 ± 3	7
6	C_6-NBD-PC	*N*-SRH-PE	−	69 ± 1	30 ± 2	70 ± 3	7
	Symmetric Vesicles:[c] Exchangeable Acceptor[d]						
7	*N*-NBD-PE	*N*-LRH-MLPE	−	57 ± 1	22 ± 3	57 ± 3	7
8	*N*-NBD-PE	*N*-LRH-MLPE	+	54 ± 1	21 ± 4	66 ± 7	12
9	*N*-NBD-PE	*N*-LRH-MLPE	−	55 ± 1	31 ± 4	46 ± 5	7
10	*N*-NBD-PE	*N*-LRH-MLPE	+	51 ± 6	17 ± 2	67 ± 5	12
11	*N*-NBD-PE	*N*-SRH-SPC(S)	−	54 ± 1	21 ± 4	57 ± 7	7
12	*N*-NBD-PE	*N*-SRH-SPC(S)	+	51 ± 1	21 ± 2	67 ± 2	12
13	*N*-NBD-PE	*N*-SRH-SPC(D)	−	53 ± 1	17 ± 3	69 ± 6	7
14	*N*-NBD-PE	*N*-SRH-SPC(D)	+	47 ± 1	21 ± 2	60 ± 2	12
	Asymmetric Vesicles:[c] Acceptor in Outer Leaflet Only[d,e]						
15	*N*-NBD-PE	*N*-LRH-MLPE	−	54 ± 1	24 ± 3	59 ± 2	13
16	*N*-NBD-PE	*N*-LRH-MLPE	+	45 ± 3	35 ± 3	67 ± 3	14
17	*N*-NBD-PE	*N*-LRH-MLPE	−	56 ± 6	23 ± 2	70 ± 3	13
18	*N*-NBD-PE	*N*-SRH-SPC(S)	−	51 ± 1	23 ± 4	59 ± 3	13
19	*N*-NBD-PE	*N*-SRH-SPC(S)	+	42 ± 1	34 ± 2	67 ± 2	14
20	*N*-NBD-PE	*N*-SRH-SPC(D)	−	49 ± 1	24 ± 3	58 ± 5	13
21	*N*-NBD-PE	*N*-SRH-SPC(D)	+	39 ± 1	31 ± 2	65 ± 2	14

[a] Uncertainties given are determined by the fitting routine from the second derivative of χ^2 with respect to the parameter (see Materials and Methods). [b] Presence or absence of DOPC vesicles at 70-fold excess. [c] Initial distribution of acceptor. [d] For exchangeable acceptors in the +DOPC condition, acceptor in the outer leaflet is diluted 70×. [e] Since all of the acceptor is initially in the outer leaflet in asymmetric vesicles and since addition of (DOPC) vesicles dilutes the concentration 70×, there is very little transfer in the +DOPC case, resulting in data which are difficult to fit.

the amount of energy transfer (Figure 4A; Table I, experiment 3). Similar results were obtained with the *N*-SRH-PE (Table I, experiments 4 and 5). A quite different situation is shown in Figure 4B (Table I, experiments 7–10). Here, the donor is again *N*-NBD-PE and the acceptor is *N*-LRH-MLPE, both being added to the lipid-forming solution. In this situation, when a 70-fold excess of DOPC vesicles was added, energy transfer decreased to an extent consistent with a 70-fold decrease in the concentration of *N*-LRH-MLPE in the outer leaflet. That is, data in the +DOPC case do not fit well to eq 6, but rather to eq 11. This demonstrates the exchangeability of *N*-LRH-MLPE, as well as its inability to undergo transbilayer movement. Similar results were obtained with the *N*-SRH-SPC (Table I, experiments 11–14). Asymmetric vesicles were also obtained by the addition from the aqueous phase of *N*-LRH-MLPE (Table I, experiments 15–17) to preformed vesicles or *N*-SRH-SPC (Figure 4C; Table I, experiments 18–21) containing *N*-NBD-PE. Here, the acceptor was assumed to be exclusively in the outer leaflet, and the data were fitted to eq 13. Consistent with the absence of acceptor in the inner leaflet, addition of excess DOPC vesicles (Figure 4C) nearly eliminated energy transfer, requiring the data to be fit by eq 14. Note that in Figure 4 the acceptor concentrations shown refer to the initial (i.e., −DOPC) condition.

We also considered transfer in symmetrically labeled vesicles between C_6-NBD-PC and *N*-SRH-PE (Table I, experiment 6).

Discussion

In this paper, we have introduced two new rhodamine-labeled lipid analogues, *N*-LRH-MLPE and *N*-SRH-SPC. Both probes could be introduced into membranes from the aqueous phase and the addition of excess DOPC vesicles depleted the fluorescence from the outer leaflet of labeled vesicles, demonstrating the exchangeability of these probes between vesicle populations. The observation that excess DOPC depletes these analogues from only the outer leaflet demonstrated that these analogues do not undergo rapid transbilayer movement. The internal quantitative consistency of the fits to the energy transfer equations comparing symmetric and asymmetric acceptor cases supports the assumption that addition of these analogues to the membrane-forming solution results in equal distribution between leaflets.

In Table II we have averaged the separate determinations of R_0 for the various donor–acceptor pairs used in these experiments. A self-consistent set of R_0 values is obtained with uncertainties <10%. These values are seen to depend most strongly upon the acceptor fluorophore *and* upon the lipid to which it is conjugated. In the case where identical acceptor (*N*-SRH-PE), but different donors (C_6-NBD-PC vs *N*-NBD-PE), were compared, the same R_0 values were obtained within experimental error. These R_0 values differ by as much as 30% from values predicted spectroscopically. This supports our contention that there are too many sources of potential error and intrinsic assumptions which must be made to calculate R_0 accurately using eq 3 and that a more accurate approach is to calculate it from energy transfer data directly (ultimately eq 2).

In Table II we have averaged the separate determinations of distances of closest approach from Table I for the various donor–acceptor pairs. These parameters of R_0 and distances of closest approach enable us to calculate the dependence of transfer efficiency upon acceptor concentration under conditions of all-cis or all-trans transfer (E_T^{cis} and E_T^{trans}) appropriate for each of the donor–acceptor pairs (Figure 5). Note that here the concentration of acceptor is given as mole fraction total lipid. We see that none of the acceptor lipid analogues are "half-bilayer quenchers". For each of the pairs considered, significant transfer is observed both within a leaflet and between leaflets.

Table II: Positions of Fluorophores Determined from Energy Transfer Measurements[a,b]

donor	acceptor	experiments from Table I averaged	R_0 (Å)	distances of closest approach: cis (Å)	distances of closest approach: trans (Å)	position from bilayer center, a = 0 model: NBD (Å), x	position from bilayer center, a = 0 model: RH (Å), y	position from bilayer center, $a = d_{cis}$ model: NBD (Å)	position from bilayer center, $a = d_{cis}$ model: RH (Å)
C_6-NBD-PC	*N*-SRH-PE	6	69 ± 1	30 ± 2	70 ± 3	20 ± 2	50 ± 2	35 ± 1	35 ± 1
N-NBD-PE	*N*-SRH-PE	4, 5	73 ± 3	37 ± 7	73 ± 10	18 ± 6	55 ± 6	37 ± 4	37 ± 4
N-NBD-PE	*N*-LRH-PE	1, 2, 3	66 ± 1	21 ± 4	62 ± 3	21 ± 3	42 ± 3	31 ± 2	31 ± 2
N-NBD-PE	*N*-LRH-MLPE	7–10, 15–17	53 ± 4	25 ± 3	62 ± 4	19 ± 3	43 ± 3	31 ± 2	31 ± 2
N-NBD-PE	*N*-SRH-SM(S)	11, 12, 18, 19	50 ± 1	25 ± 3	63 ± 4	19 ± 3	44 ± 3	32 ± 2	32 ± 2
N-NBD-PE	*N*-SRH-SM(D)	13, 14, 20, 21	47 ± 1	23 ± 3	63 ± 4	20 ± 3	43 ± 3	32 ± 2	32 ± 2

[a] Uncertainties determined by error propagation assuming independent samples. [b] All distances are given in angstroms.

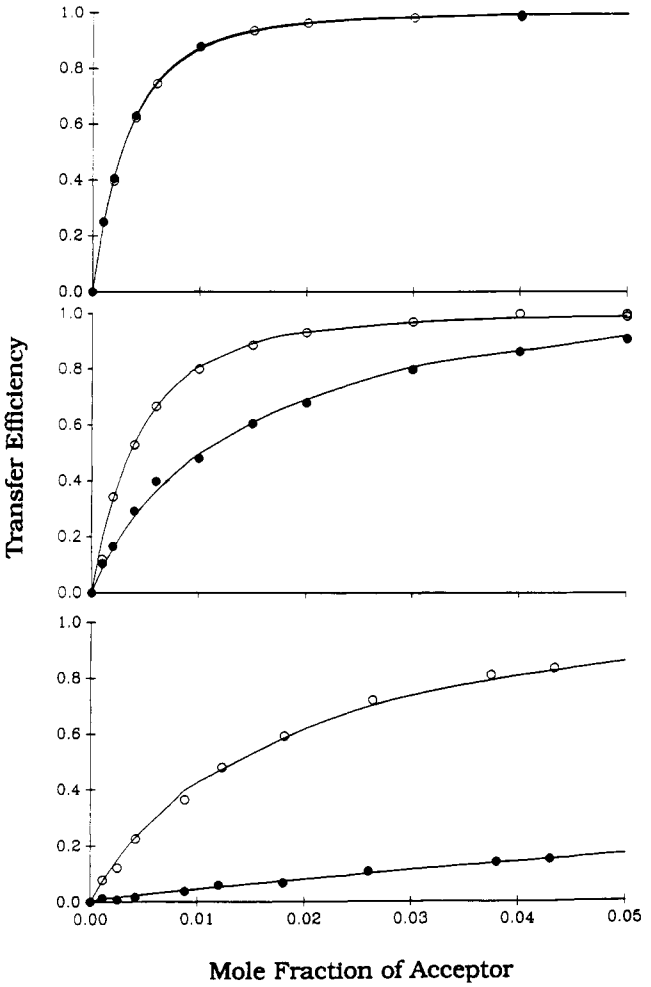

FIGURE 4: E_T vs acceptor concentration for the three types of experiments done, (○) without and (●) with excess unlabeled DOPC vesicles. Solid lines show theoretical fits to the data. (A, top) Symmetric vesicles with *N*-NBD-PE (donor) and nonexchangeable *N*-LRH-PE (acceptor). Referring to Table I data, ○ is exp no. 2 and ● is exp no. 3. Both cases were fit to eq 7. (B, middle) Symmetric vesicles with *N*-NBD-PE (donor) and *N*-LRH-MLPE (acceptor): (○) exp no. 7 (data fit to eq 7); (●) exp no. 8 (data fit to eq 12). (C, bottom) Asymmetric vesicles with *N*-NBD-PE (donor) and *N*-SRH-SPC (acceptor): (○) exp no. 20 (data fit to eq 13); (●) exp no. 21 (data fit to eq 14).

In an experiment where acceptor is confined to a single leaflet while the donor is distributed in an unknown way between leaflets, the transfer would be a linear combination of all-cis and all-trans transfer. Equation 13 represents the special case of equal donor distribution with all acceptors in the outer leaflet. The more general case would be given by

$$E_T = (1 - \alpha)E_T^{trans} + (\alpha)E_T^{cis} \quad (15)$$

where α is the fraction of donor in the same leaflet as the acceptor. Using eq 15, the results of Figure 5 can be used to

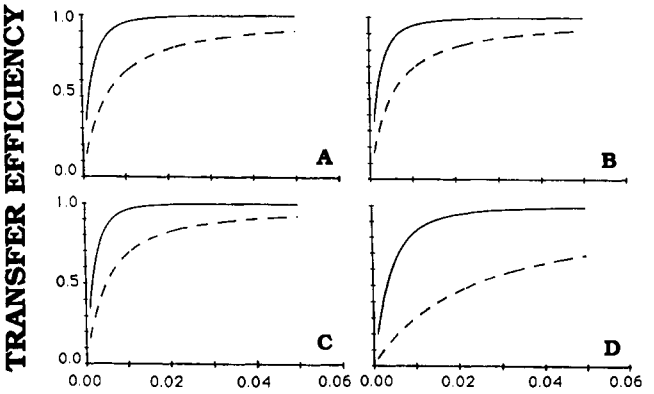

FIGURE 5: Use of FRET to determine the transbilayer distribution of C_6-NBD-PC. Parameters from Table II were used to generate curves for all-cis (—) and all-trans (- - -) transfer between (A) C_6-NBD-PC and *N*-SRH-PE, (B) *N*-NBD-PE and *N*-SRH-PE, (C) *N*-NBD-PE and *N*-LRH-PE, and (D) *N*-NBD-PE and *N*-LRH-MLPE or *N*-SRH-SPC.

calculate the transbilayer distribution of the donor in any intermediate case.

Our energy transfer results can also be used to obtain information about the localization of the fluorescent moieties of these lipid analogues relative to the bilayer center.

According to eqs 11a and 11b, the distances of closest approach for cis and trans transfer, d_{cis} and d_{trans}, are given by

$$d_{cis} = [a^2 + (y - x)^2]^{1/2} \quad (16a)$$

$$d_{trans} = y + x \quad (16b)$$

Absolute determination of the distances of the donor and acceptor, x and y, from the bilayer center requires an independent measure of the in plane steric hindrance distance a. In the absence of such a determination, our data enable us to set limits on x and y, since for $y - x$ to be real, a can range only from 0 to d_{cis}. Values calculated for these two extremes are given in Table II. Transfer from *N*-NBD-PE to *N*-LRH-PE, *N*-LRH-MLPE, or *N*-SRH-SPC gives the same values for d_{cis} and d_{trans} and shows that the rhodamines lie between 42 and 31 Å from the bilayer center with the NBD lying between 19 and 31 Å. Transfer between *N*-NBD-PE and *N*-SRH-PE shows that the rhodamine of that probe is between 55 and 37 Å from the bilayer center and the NBD is between 18 and 37 Å. The appropriate distance from the bilayer center to the lipid phosphates is ~19 Å. *These data thus tell us that the rhodamine fluorophores are all well above the lipid phosphates and the NBD group of N-NBD-PE is at or above the phosphate.* Since the upper limit of rhodamine position is hard to reconcile with molecular dimensions, it is likely that a is greater than zero. The assumption that a equals the intermolecular distance between lipid head groups (8.4 Å) has little effect on y. It thus seems likely that a is large and

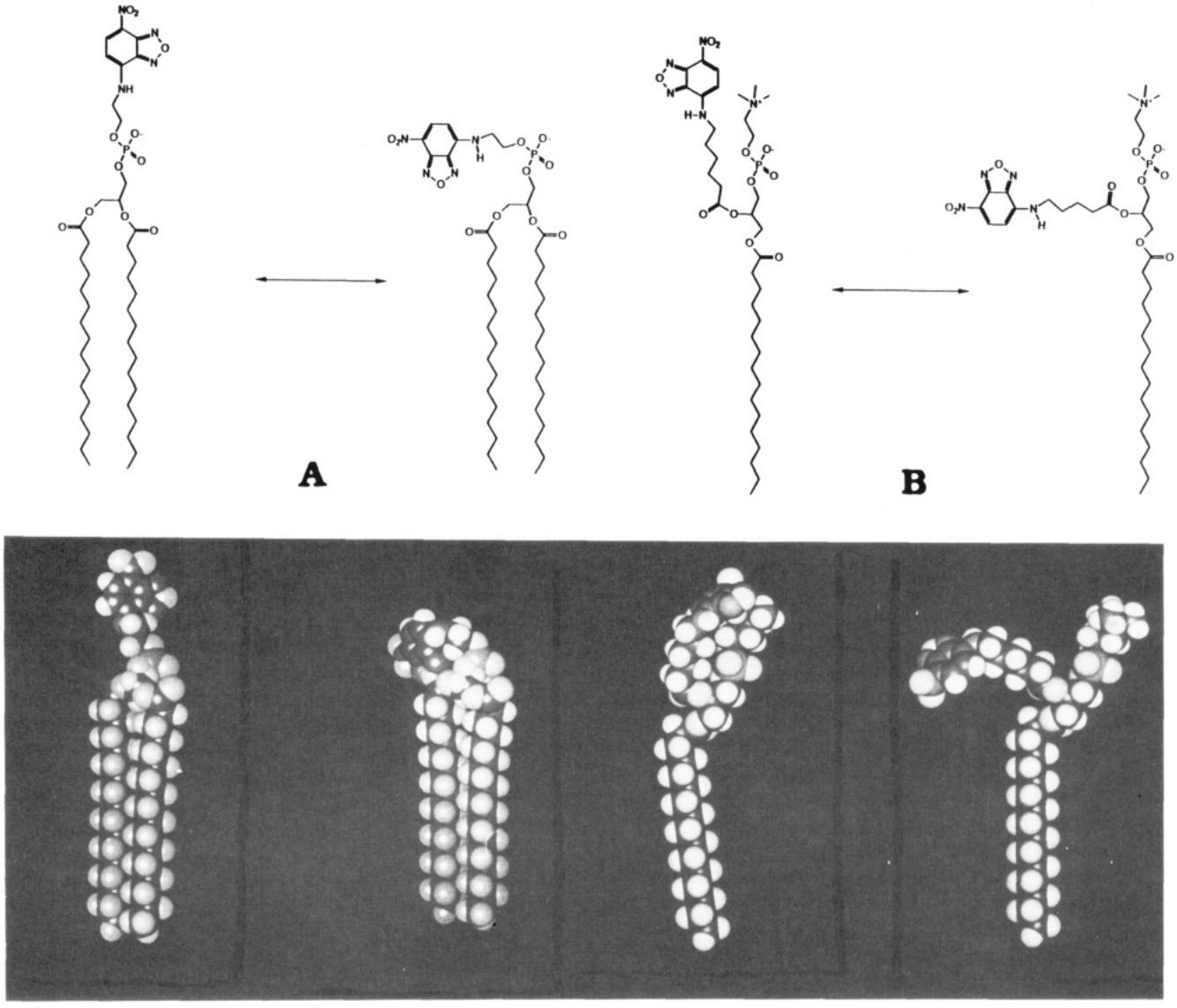

FIGURE 6: Structures of *N*-NBD-PE (A) and C_6-NBD-PC (B) showing how free rotation around a single bond could result in a large variation in the NBD positions.

that the lower limit for the rhodamines and the upper limit of the distance from the bilayer center for the NBD are more realistic. Three-dimensional structures consistent with these conclusions were generated by an energy minimization program and are shown in Figure 1.

Transfer between C_6-NBD-PC and *N*-SRH-PE places the rhodamine between 50 and 35 Å and the NBD between 20 and 35 Å from the bilayer center. These values for the rhodamine are consistent with the values determined using *N*-NBD-PE as the donor. Thus, the NBD of C_6-NBD-PC, like that of *N*-NBD-PE, appears to be at or above the lipids phosphates. This conclusion is independent of the value of a since, according to eq 16b, d_{trans} is independent of a. The differences in the d_{trans} for *N*-NBD-PE and C_6-NBD-PC are equal to the difference in x. Thus, the NBD group in C_6-NBD-PC is 3 ± 10 Å below the NBD group in *N*-NBD-PE (see Table II).

These calculations may be compared to two other determinations of the position of NBD groups on C_6-NBD-PC and *N*-NBD-PE. Connor and Schroit (1987) estimated the NBD group on C_6-NBD-PC to be about 6 Å from the bilayer center while Chattopadhyay and London (1987) determined that the NBD group of C_6-NBD-PC and *N*-NBD-PE are to be about 12 and 14 Å from the bilayer center, respectively.

Both our data and those of Chattopadhyay and London (1987) contradict the conclusion of Connor and Schroit (1987) that the NBD group of C_6-NBD-PC is buried deeply in the hydrocarbon core of the bilayer. Connor and Schroit (1987) used a simple nearest neighbor theory to fit their data. Such an approach is, at best, approximate (Koppel et al., 1979).

Our data are in agreement with Chattopadhyay and London (1987) in that we both find that the NBD groups in C_6-NBD-PC and *N*-NBD-PE are, roughly speaking, at the same level relative to the bilayer center. Our data do, however, appear to disagree somewhat, since we find both probes to be at or above the level of the phosphates, while Chattopadhyay and London (1987) place them at or below the carbonyls. Chattopadhyay and London (1987) have pointed out that the precise meaning of distances of closest approach and position may depend upon the technique used. FRET measures an average position weighted as $1/r^6$. As shown in Figure 6, rotation about a single bond can bring the NBD groups of C_6-NBD-PC and *N*-NBD-PE from the positions indicated by our data to those indicated by Chattopadhyay and London (1987). Such a rotation might be expected to occur relatively freely. Quenching of NBD fluorescence by a spin probe with very small R_0 within the bilayer would be heavily biased in favor of NBD molecules near the surface. To a lesser degree

(because of the larger R_0), our data would favor NBD molecules farther from the surface, that is, nearer the rhodamines. By detailed and more rigorous analysis, one can potentially use this bias to one's favor and determine not only the mean fluorophore position but the probability distribution of positions as well (Cantor & Pechukas, 1971; Grinvald et al., 1972).

Conclusions

In conclusion, we have

(1) Determined the corrected spectra and R_0 values appropriate for fluorescence resonance energy transfer measurements between a series of rhodamine and NBD labeled lipid analogues.

(2) Introduced two new fluorescent lipid analogues, *N*-LRH-MLPE and *N*-SRH-SPC, which exchange readily across the aqueous phase but do not flip rapidly between bilayer leaflets.

(3) Demonstrated that these exchangeable rhodamine lipid analogues effectively quench NBD lipid analogue fluorescence in lipid bilayer membranes by nonradiative fluorescence resonance energy transfer.

(4) Established the parameters of energy transfer quenching of NBD lipid analogue fluorescence, demonstrating that all of the acceptor (rhodamine) lipid analogues considered (exchangeable and nonexchangeable) quench the fluorescence of donor (NBD) lipids in the opposite (trans) leaflet of the bilayer membrane, providing a theoretical basis for future use of these probes in studying NBD lipid transbilayer distribution and transport. Therefore, none of them can be considered "half-bilayer quenchers".

(5) Set limits on the positions of the donor (NBD) and acceptor (rhodamine) fluorphores relative to the bilayer center using energy transfer data. The rhodamine probes are all well above the lipid phosphates, and the NBD groups of *N*-NBD-PE and C_6-NBD-PC are at or above the phosphates.

Acknowledgments

We thank Dr. Michael Koval for help in the initial phases of this work, Ms. Ona Martin for technical assistance, and Dr. Richard Cardullo for critical reading of the manuscript. We thank Christine McKinnon, Sandra Johnson, and Rebecca Bell for their invaluable assistance in the preparation of the manuscript. We also thank the Howard Hughes Research Laboratory of the Carnegie Institution of Washington for use of their molecular graphics facility.

References

Abramowitz, M., & Stegun, I. A. (1965) *Handbook of Mathematical Functions*, U.S. Government Printing Office, Washington, D.C.

Baird, B., & Holowka, D. (1988) *Spectroscopic Membrane Probes* (Loew, L. M., Ed.) Vol. I, pp 93–116, CRC Press, Boca Raton, FL.

Bevington, P. R. (1969) *Data Reduction in the Physical Sciences*, McGraw-Hill, Inc., New York.

Cantor, C. R., & Pechukas, P. (1971) *Proc. Natl. Acad. Sci. U.S.A. 68*, 2099–2101.

Cardullo, R. A., Agrawal, S., Flores, C., Zamecnik, P. C., & Wolf, D. E. (1988) *Proc. Natl. Acad. Sci. U.S.A. 85*, 8790–8794.

Chattopadhyay, A. (1990) *Chem. Phys. Lipids 53*, 1–15.

Chattopadhyay, A., & London, E. (1987) *Biochemistry 26*, 39–45.

Connor, J., & Schroit, A. J. (1987) *Biochemistry 26*, 5099–5105.

Dale, R. E., Nouros, J., Roth, S., Edidin, M., & Brand, L. (1981) in *Fluorescent Probes* (Beddard, G. S., & West, M. A., Eds.) pp 159–181, Academic Press, London.

Ethier, M. F., Wolf, D. E., & Melchior, D. L. (1983) *Biochemistry 22*, 1178–1182.

Fleming, P. J., Koppel, D. E., Lau, A. L. Y., & Strittmatter, P. (1979) *Biochemistry 18*, 5458–5463.

Förster, T. (1948) *Ann. Phys. 2*, 55–75.

Fung, B, K.-K., & Stryer, L. (1978) *Biochemistry 17*, 5241–5248.

Grinvald, A. E., Haas, E., & Steinberg, I. Z. (1972) *Proc. Natl. Acad. Sci. U.S.A. 69*, 2273–2277.

Hiratsuka, T., & Kato, T. (1987) *J. Biol. Chem. 262*, 6318–6322.

Hope, M. J., Bally, M. B., Webb, G., & Cullis, P. R. (1985) *Biochim. Biophys. Acta 812*, 55–65.

Kenner, R. A., & Aboderi, A. A. (1971) *Biochemistry 10*, 4433–4440.

Kleinfeld, A. M. (1985) *Biochemistry 24*, 1874–1882.

Koppel, P. E., Fleming, P. J., & Strittmatter, P. (1979) *Biochemistry 18*, 5450–5457.

Kremer, J. M. H., Esker, M. W. J., Pathmamanoharan, C., & Wiersema, P. H. (1977) *Biochemistry 17*, 3932–3935.

Loew, L. M., Ed. (1988) *Spectroscopic Membrane Probes*, Vol. 1, p 227, CRC Press, Boca Raton, FL.

Martin, O. C., & Pagano, R. E. (1987) *J. Biol. Chem. 262*, 5890–5898.

Mavrodineau, R., Shulz, J. I., & Menis, O., Eds. (1973) *Accuracy in Spectrophotometry and Luminescence*, NBS U.S. Department of Commerce publication no. 378.

Mayer, L. D., Hope, M. J., Cullis, P. R., & Janoff, A. S. (1985) *Biochim. Biophys. Acta 817*, 193–196.

Nichols, J. W., & Pagano, R. E. (1982) *Biochemistry 21*, 1720–1726.

Nichols, J. W., & Pagano, R. E. (1983) *J. Biol. Chem. 258*, 5368–5371.

Pagano, R. E. (1989) *Methods in Cell Biology*, Vol. 29, pp 75–85, Academic Press, Inc., San Diego, CA.

Pagano, R. E., & Longmuir, K. J. (1985) *J. Biol. Chem. 260*, 1909–1916.

Pagano, R. E., & Sleight, R. G. (1985) *Science 229*, 1051–1057.

Pagano, R. E., Longmuir, K. J., Martin, O. C., & Struck, D. K. (1981a) *J. Cell Biol. 91*, 872–877.

Pagano, R. E., Martin, O. C., Schroit, A. J., & Struck, D. K. (1981b) *Biochemistry 20*, 4920–4927.

Parker, C. A. (1968) *Photoluminescence of Solutions*, p 267, Elsevier, Amsterdam.

Rouser, G., Fleischer, S., & Yamamoto, A. (1970) *Lipids 5*, 494–512.

Struck, D. K., & Pagano, R. E. (1980) *J. Biol. Chem. 255*, 5404–5410.

Struck, D. K., Hoekstra, D., & Pagano, R. E. (1981) *Biochemistry 20*, 4093–4099.

Tao, T., & Morris, E. P. (1983) *Biochemistry 22*, 3059–3066.

Taylor, D. L., Reidler, J., Spudich, J. A., & Stryer, L. (1981) *J. Cell Biol. 89*, 362–367.

Uster, P. S., & Pagano, R. E. (1986) *J. Cell Biol. 103*, 1221–1234.

Weast, R. C. D., Astle, M. J., & Beyer, W. H., Eds. (1987) *CRC Handbook of Chemistry and Physics*, 68th ed., p E372, CRC Press, Boca Raton, FL.

Wells, B. D., & Cantor, C. R. (1977) *Nucleic Acids Res. 5*, 1667–1680.